

# Modeling the differential susceptibility by Lorentzians

Alexej Perevertov

## AFFILIATION

Institute of Physics of the Czech Academy of Sciences, Department of Magnetic Measurements and Materials, 18200 Prague, Czech Republic

## ABSTRACT

The idea to extract information on magnetically different phases from magnetic measurements is very attractive and many efforts have been made in this area. One of the most popular direction is to use the Preisach model formalism to analyze the 2D Preisach distribution function (PDF) obtained either from first order reversal curves (FORC) or minor loops. Here we present an alternative a much simpler procedure – the analysis of the derivative of the saturation magnetization loop, the differential susceptibility curve. It follows the Lorentzian shape with very high accuracy for ferromagnetic polycrystalline materials. This allows decomposing any differential susceptibility curve of a complex multi-phase material into individual components representing different magnetic phases by Lorentzian peaks – in the same way as it is done in X-ray analysis of materials. We show that the minor differential susceptibility curves also have the Lorentzian shape that can facilitate calculation of the Preisach distribution function from the experimental curves and reduce noise in the resulting PDF.

## I. Introduction

Magnetic hysteresis loop,  $M(H)$  loop shows the relationship between magnetization,  $M$  and the applied magnetic field,  $H$ . It is a subject of intensive study for the last 150 years since it characterizes magnetic properties of a material. The  $M(H)$  loop shape changes with the field amplitude increase – the coercive force,  $H_C$  and the maximum differential susceptibility (DS) increase. After reaching a certain value of the field amplitude,  $H_C$  and the shape of DS do not change anymore [1]. This moment is called the technical saturation. With the further field increase the magnetization grows in a fully reversible way, mostly by the magnetic moments rotation from the crystal magnetic easy axes toward the applied field direction. The field necessary to orient all the magnetic moments in a polycrystalline material is at least two orders larger comparing to the technical saturation field. In most cases investigators work with the technical saturation  $M(H)$  loops, called major hysteresis loops. The loops with smaller amplitudes are called “minor loops” and their shape strongly depends on the magnetic prehistory.

The modeling of  $M(H)$  loops of materials is very important not only for applications but also from the physical point of view to understand and predict evolution of magnetic properties with change of the composition, temperature, stress etc. There are hundreds of works devoted to modeling the hysteresis loops [2-10]. The model should be as simple as possible and at the same time it has to describe very accurately experimental magnetization curves. Ideally, it should be a simple analytical function with a small number of parameters. At present the most known and popular models are the Preisach and the Jiles-Athertone models of hysteresis that are quite complex. Also new models were introduced recently, some of them are very complex with a large number of parameters [5,11-12]. For representation of the major hysteresis loops, anhysteretic magnetization curves and 2D Preisach distribution functions (PDF) a number of analytical functions have been tried for the last decades [13-25].

A usual simple  $M(H)$  curve has an “S” shape, the mathematical functions with that shape are called “sigmoid”. There exist a large number of analytical sigmoid functions resembling real measured hysteresis loops. For a simple one-magnetic-phase hysteresis curve the main criterion is the saturation at infinitely large fields. The hysteresis curve derivative – the differential susceptibility (DS) for one-phase magnetic materials should be a one-peak function. There are many sigmoid functions: the ordinary arctangent, the hyperbolic tangent, the Gudermannian function, the error function, the generalized logistic function and algebraic functions and so on. The examples of several simple sigmoid functions are presented in Fig.1. All of them resemble real experimental  $M(H)$  curves. If one accepts 5-10% deviation of the magnetization from the experimental curve, then any of these functions can be successfully used for magnetic

hysteresis modeling. The difference is in the approaching saturation, which is much slower for arctangent and Langevin functions. The derivative of a rectangular  $M(H)$  loop is the delta-function.

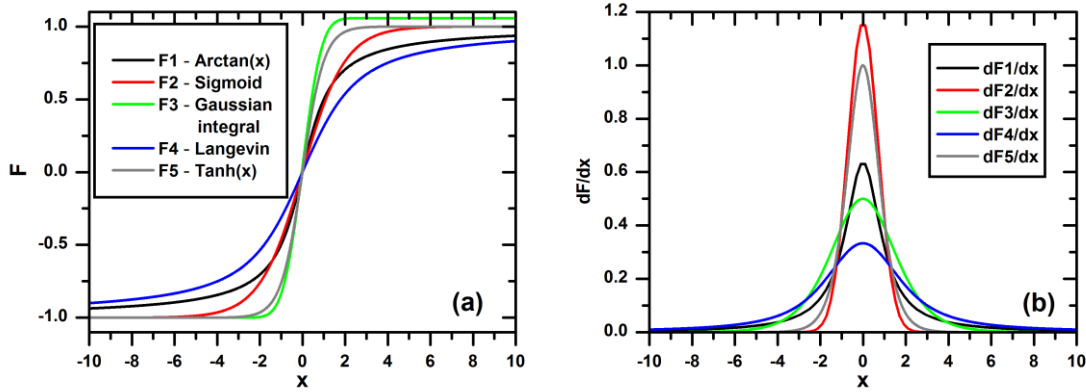


**FIG.1.** Several analytical functions representing ascending magnetization curves (a) and their derivatives - the differential susceptibility. F1 is the arctangent function, F2 – the sigmoid function, F3 – the integral of Gaussian, F4 – the Langevin function and F5 – the hyperbolic tangent. All the functions are scaled and biased to the  $\pm 1$  magnetization range.

In 1990s many investigators believed that the Preisach model formalism will be used similar to the Fourier analysis to extract information about individual magnetic phases in the material. It was believed that 2D Preisach distribution function (PDF) will have additional peaks comparing to traditional susceptibility curves. We have found that it did not work in this way. For  $n$ -peak differential susceptibility there will be  $n$ -peak PDF. The additional information that can bring minor loops or the first order reversal curves (FORC) – magnetostatic interaction between magnetic phases that leads to negative areas in PDF [26]. We have found that in this case the direct analysis of the set of minor susceptibility curves is sufficient to discover even the smallest interaction without need to calculate the PDF [26]. The PDF obtained experimentally is usually very noisy and the measurement and data evaluation procedures are complex. We also have shown that the PDF can be obtained directly from the differential susceptibility (DS) curves without need to start from the integral quantity – the  $M(H)$  loops [26]. So we concentrated on investigation of DS curves instead of PDF since they already contain information about the number of magnetic phases in the material. In the Preisach model the DS curve of the saturated hysteresis loop is given by the distribution of the switching up fields.

In most investigations either the  $M(H)$  curves are analyzed or the second derivative – the PDF function. There are very few articles on the shape of the first derivative – DS curve. In this article we want to fill this gap. Even if the difference between the  $M(H)$  curves is hardly seen by the naked eye, the difference in the corresponding differential susceptibility curves could be very large. The first derivative – the DS curve is much more sensitive to comparing to  $M(H)$  curves and at the same is much less noisier than the second derivative – PDF, the shape of the DS curve can be studied in details.

## II. Lorentzian shape of the differential susceptibility of polycrystalline materials

For more than 20 years we collected a large number of experimental  $M(H)$  curves of polycrystalline materials like steels. In most cases we worked directly with the DS curves. We have noticed already from the beginning that the Lorentzian function always described the DS curves of steels with very high accuracy, accordingly the  $M(H)$  curves had an arctangent shape [27]. It perfectly worked in all cases – for single-phase materials with one DS peak, for materials with the second magnetically different layer and even for samples with two-peak DS due to stress-induced anisotropy. It worked for steels with the grain size from tens of microns to several centimeters, for different materials like pure iron, pure nickel, cast irons (see Fig.2) and magnetic shape memory alloys. These observations suggest that it is a general law for magnetization curve of polycrystalline materials to have the Lorentzian shape of the DS curve. As the result, the DS curves of polycrystalline ferromagnetic materials could be described with very high accuracy by a sum of Lorentzians and so the magnetic spectroscopy can be introduced based on the decomposition of the DS curve of a material into Lorentzian peaks in the same way as it is commonly done in X-ray analysis of materials.

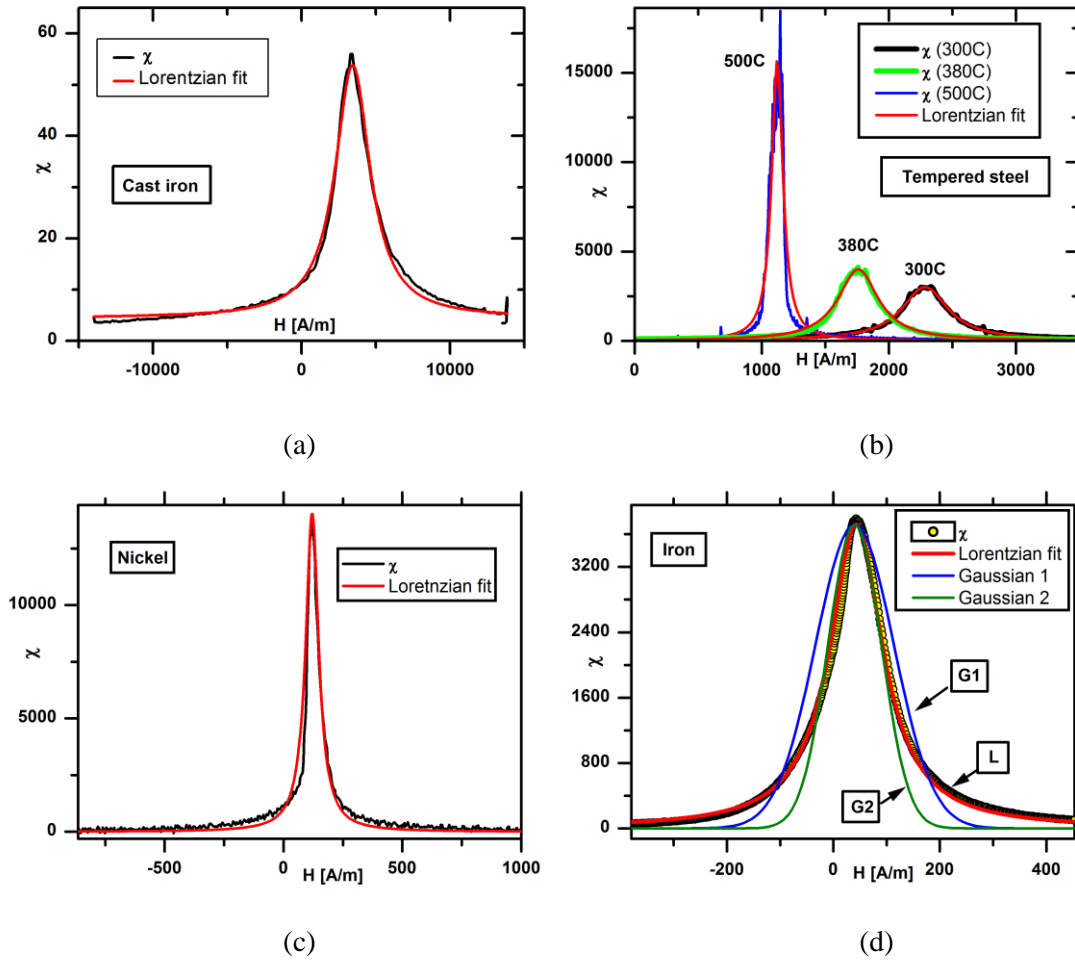


**FIG.2.** Differential susceptibility curves,  $\chi(H)$  and corresponding Lorentzian fits of cast iron (a), quenched and tempered for one hour at 300°C, 380°C and 500°C spring steels (b) [s1], pure nickel (c) and pure iron (d). In (d) also two Gaussian fits are shown. The Gaussian 1 – the same area under the curve and the maximum as of the experimental susceptibility curve. The Gaussian 2 – the same maximum value and the same half-width.

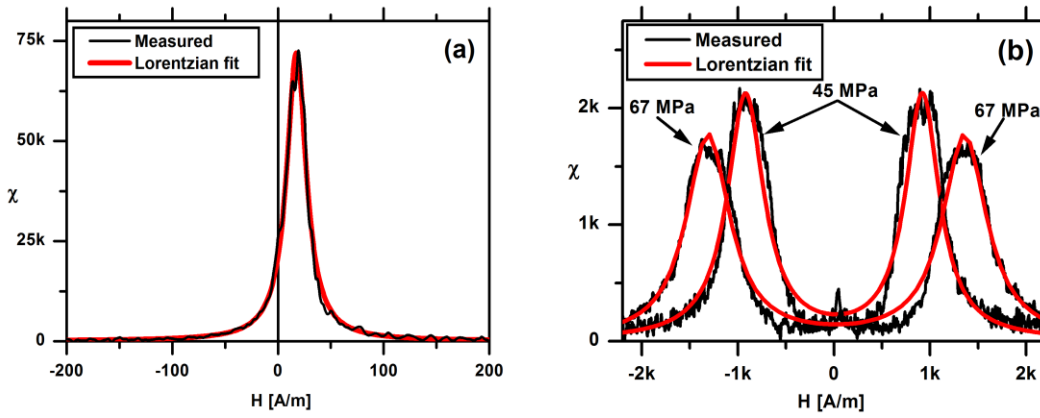
The arctangent function for the ascending branch of the  $M(H)$  loop and its derivative – the Lorentzian are given below:

$$M(H) = (2/\pi) M^{SAT} \arctan(a[H-H_C])$$

$$\chi(H) = dM/dH = (2/\pi) a M^{SAT} / (1 + a^2(H-H_C)^2), \quad (1)$$

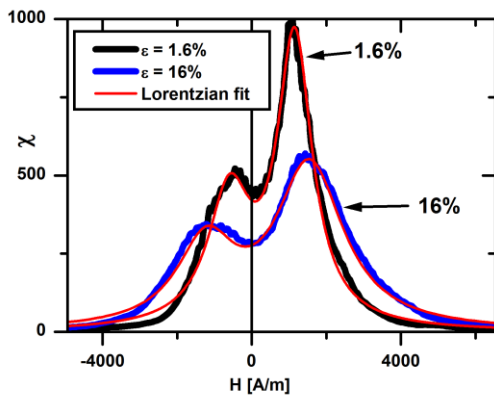
Where  $M^{SAT}$  is the saturation magnetization,  $H$  – internal magnetic field,  $\chi$  – the differential susceptibility (DS),  $H_C$  – the coercive field.

In Fig.3 the DS curves for Goss-textured Fe-3%Si steel sheets without stress and under applied elastic compressive stress of 45MPa and 67MPa are shown. The DS of compressed samples was modeled by a sum of two Lorentzians. It is seen that the agreement with experimental curves is excellent. The average grain size was about 10 mm, the details of measurements can be found in [28]. The agreement was very good for all stresses above 5-10 MPa. Below 10 MPa there is a transition from one-peak to two-peak DS and so the DS curve is the combination of the zero-stress one-peak and two peaks by the domain reorientations.

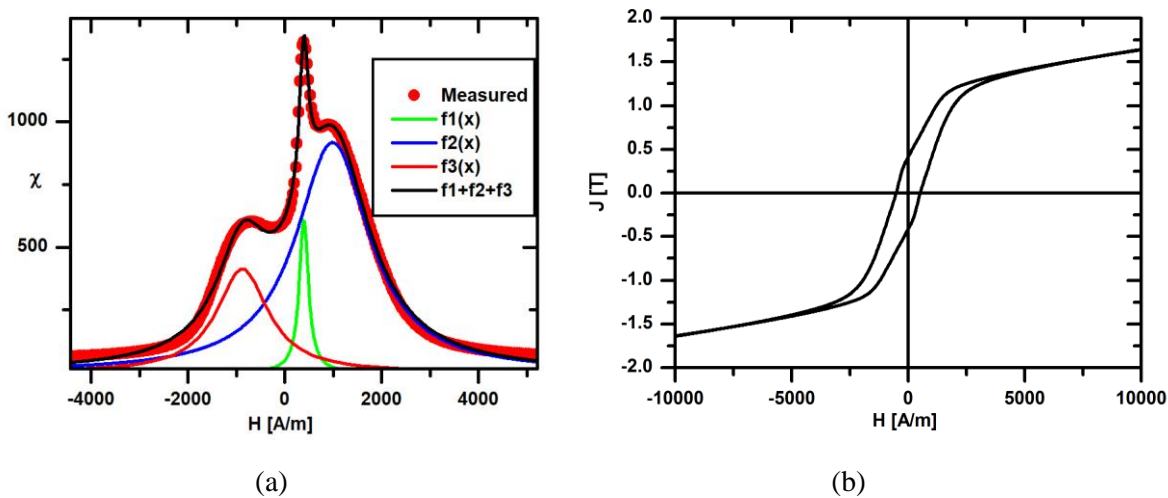


**FIG.3.** Differential susceptibility curves  $\chi(H)$  for the Goss textured Fe-3%Si steel without stress (a) and under 45MPa and 67MPa compressive stress (b).

The DS of plastically deformed low-carbon steel from our previous work [29] could also be fitted by the sum of two Lorentzians with the same accuracy (see Fig.4). Moreover, in that work we machined several samples to make them flatter and thus to reduce air gaps between the sample and the magnetizing yoke. As the result, we got an unwanted thin decarburized surface layer, which was much softer magnetically comparing to the bulk. The DS of such samples consists of three peaks – two of the bulk by magnetic domains reorientations (see Fig.3(b)) due to stress-induced anisotropy [28] and the third one by a thin decarburized layer. In Fig.5 the experimental DS curve of such a sample is modeled by the sum of three Lorentzians. The agreement is excellent, the experimental and measured DS curves are practically indistinguishable.



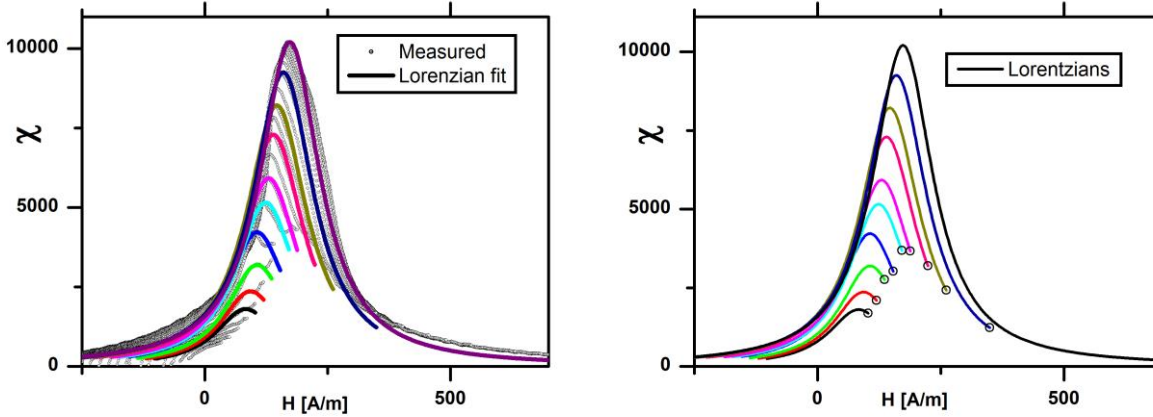
**FIG.4.** Differential susceptibility curves  $\chi(H)$  of plastically deformed low-carbon steel and two-Lorentzians fit.



**FIG.5.** Three-peaks  $\chi(H)$  (a) for a deformed low-carbon steel [29] and corresponding magnetic hysteresis loop (b) measured along the hard axis. Two peaks at higher fields are due to magnetic domains reorientation from the field direction to that perpendicular to it and back. The third thin peak is given by a thin magnetically soft decarburized layer. The measured curve is represented as a sum of three Lorentzians:  $F(x) = f1(x)+f2(x)+f3(x)$ .

Above we considered only major differential susceptibility curves. What about the minor curves – do they also have the Lorentzian shape? In Fig.6 the set of minor DS curves measured on the low-carbon steel (ČSN 12014) after demagnetization. The minor DS curves have the Lorentzian shape with the same width (see the Table 1). The curves are asymmetric because the magnetic field range is symmetric with respect to the zero field, not with respect to the minor loop coercivity  $H_C$ . According to the Preisach model, the final points of the minor curves should give the virgin curve [30].

Fitting the minor DS curves by Lorentzians can greatly reduce noise of the calculated PDF for the Preisach modeling. The shift of the minor DS curve with the field amplitude is usual for steels and is connected with magnetostatic interaction with different material regions commonly treated in the Preisach modeling as the mean-field effect [26]. The dependence of the DS curve position,  $H_C$  on the field amplitude,  $H^{MAX}$  can reveal the information on the magnetostatic interaction between different magnetic phases in a material.



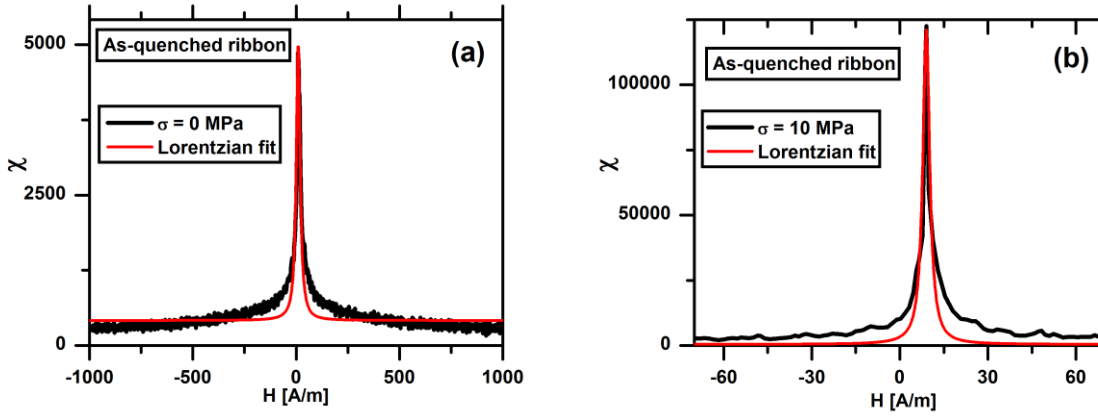
**FIG.6.** Minor differential susceptibility curves and corresponding Lorentzians for a low-carbon steel.

Table 1. Lorentzian parameters for the minor differential susceptibility curves.  $H^{MAX}$  is the minor loop amplitude.

$H^{MAX}$ (A/m)	$(2/\pi) a M^{MAX}$	$a$ (m/A)	$H_C$ (A/m)
103	1808	0.116	83
119	2364	0.116	93
136	3192	0.116	107
153	4222	0.116	107
170	5156	0.116	124
188	5924	0.116	130
223	7292	0.116	140
260	8217	0.116	147
350	9252	0.116	160
880	10202	0.116	173

### III. Discussion

We see that the Lorentzian function describes DS of polycrystalline steels with very high accuracy for non-oriented materials and for grain-oriented ones. Also it gives an excellent agreement with experimental curves of quenched and tempered steels [31]. From other side, the shape of DS of amorphous ribbons is different from the Lorentzian (See Fig.7). We have tried a number of ribbons with different compositions and after different heat treatments and the agreement was never as good as for polycrystalline materials. In the polycrystalline materials at low and moderate fields the magnetization process is realized through the magnetic domains motion. The grains have the cubic anisotropy and the magnetic moments are along one of three easy axes. The domains move relatively freely inside grains and the main obstacles are grain boundaries and local defects and residual stress. In contrast, in as-quenched amorphous ribbons the anisotropy in different regions is uniaxial given by the local residual stresses [32]. In addition, we discovered that the effective field model for magnetization curves that gives very good agreement with experimental curves on differently stressed steels [28-29, 31, 33] does not work on amorphous ribbons.



**FIG.7.**  $\chi(H)$  of as-quenched amorphous ribbon for zero stress (a) and under 10 MPa tension (b).

In the polycrystalline material due to a grain misorientation from the field direction there is the demagnetizing field inside the grain proportional to the grain magnetization. Let us consider a collection of volumes/grains with the magnetization curve  $M(H)$  given by the demagnetizing factor and all demagnetizing factors being equally distributed. We assume that in each grain the internal magnetization curve (no demagnetizing fields) is rectangular – the susceptibility approaches the delta-function. Let us consider eight grains having the same high constant differential susceptibility  $\chi = 128$  in the field range  $\pm 1$ . Let us take the first grain with no demagnetizing field. The susceptibility in the second grain due to the demagnetizing field is 64 in the field range  $\pm 2$ , in the third – 32 in the field range  $\pm 4$  and so on. If we look at the sum of all susceptibilities, we see that the total susceptibility is close to the Lorentzian shape (see Fig.8).

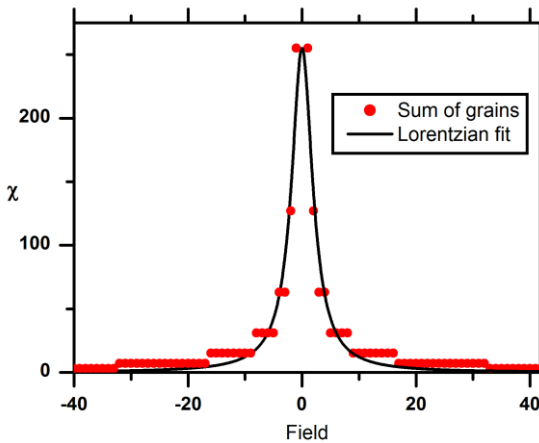


**FIG.8.** The differential susceptibility by a collection of eight grains with different demagnetizing factors.

The considerations above are just illustrative, but they give a clue how the one-peak DS curve is obtained for a polycrystalline material. To understand why  $M(H)$  curves of such materials follow the arctangent shape with a very high accuracy, 2D and 3D statistical calculations of collections of grains are necessary for different grain angle distributions.

The simplest polycrystalline material, for which the Lorentzian describes the DS with a high accuracy (see Fig.3) is a Goss-textured Fe-3%Si thin sheet. The average easy axis is along the field direction with small grains misorientation angles. The magnetic domains are oriented in each grain along the easy [001] axis closest to the applied magnetic field direction. Due to the grain misorientation demagnetizing fields appear at the grain boundaries and at the sheet surface. Supplementary domains minimize these demagnetizing fields. Removal of the supplementary domains by tensile stress (see Fig.9) increases demagnetizing fields that substantially affects the  $M(H)$  loops shape [33]. So even in this simplest case one has to include the supplementary (closure) domains and corresponding demagnetizing fields to create a realistic micromagnetic statistical model of a magnetization curve.

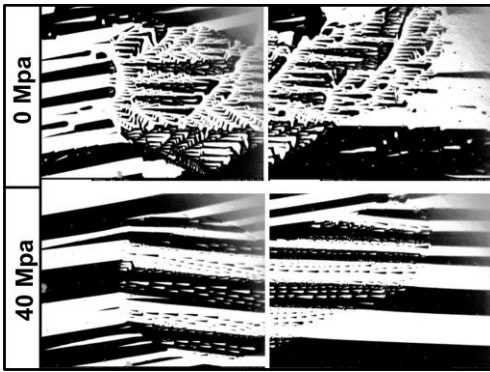


**FIG.9.** Magnetic domains in a Goss-textured Fe-3%Si thin sheet for 0 and 45 MPa tensile stress.

It is intriguing that the DS peaks of elastically and plastically deformed materials measured along the magnetically harder direction are also a sum of Lorentzians (see Fig.2 and Fig.3). We have shown that two- and three-phase hysteresis loops could be fitted by two and three Lorentzians correspondingly with excellent agreement with experimental data. The arctangent function for the magnetization curve has three parameters - the saturation magnetization, the coercivity and the magnetization slope (maximum differential susceptibility) at the coercivity. It is a simplest function with a minimum necessary number of physical parameters that surprisingly give an excellent agreement with experimental curves of polycrystalline materials. Another surprising fact is that the susceptibility is usually decomposed into the reversible and irreversible part [3-7], while the Lorentzian describes the total susceptibility ignoring separation into individual components.

#### **IV. Conclusions**

We see that the Lorentzian, which is commonly used in spectroscopy to fit the data to extract individual components could be used in the same way to extract individual magnetic components from the differential susceptibility curves. All the necessary algorithms and procedures could be taken from the optical and X-ray spectroscopy. The magnetic spectroscopy using Lorentzians could especially helpful for analysis of individual phases in multi-phase materials. Often there is a second magnetically harder phase that is hardly seen on the total curve, which by the magnetostatic interaction with the main softer phase makes the DS curve to shift to higher fields with the field amplitude increase also making the curve more and more asymmetric [26]. So, from the deviation of DS curve from the Lorentzian shape one can detect the presence of the second phase. Sometimes, the second phase is close magnetically to the first one and the DS curves of two phases are very close and can't be easily distinguished by the naked eye like the deformed layer of magnetically hard bearing steels [34]. In this case the analysis based on the search of a sum of Lorentzian peaks will be helpful. In the case of DS of a material under stress the description of magnetic properties change is reduced to just a few parameters of one or two Lorentzians.

One has to keep in mind that the model should be applied to  $M(H)$  of a material measured accurately. It is not an easy task for a yoke-sample setup if air gaps are present that produce demagnetizing fields. The toroidal or ring-shaped samples are closed magnetic circuit, but even in this "ideal" case there can be large measurement errors in  $M$  and  $H$  if the ratio of the sample thickness to the diameter is lower than 1 to 10 [35].

#### **Declaration of competing interest**

The authors have no conflicts to disclose.

#### **Data availability**

The data that support the findings of this study are available from the corresponding authors upon request.

#### **Acknowledgments**

The authors acknowledge the assistance provided by the Ferroic Multifunctionalities project, supported by the Ministry of Education, Youth, and Sports of the Czech Republic. Project No. CZ.02.01.01/00/22\_008/0004591, co-funded by the European Union.

## References

- [1] R.M. Bozorth, *Ferromagnetism*. Van Nostrand, New York (1951).
- [2] E. Della Torre, *Magnetic Hysteresis*, Wiley-IEEE Press (2005).
- [3] I.D. Mayergoyz, *Mathematical Models of Hysteresis*, Springer, New York (2003).
- [4] G. Bertotti, *Hysteresis in Magnetism*, Academic Press, San Diego, (1998).
- [5] V. Hassani, T. Tjahjowidodo and T.N. Do, A survey on hysteresis modeling, identification and control, *Mech. Syst. Signal Proc.* **49**, 209-233 (2014).
- [6] D.C. Jiles, Hysteresis models: non-linear magnetism on length scales from the atomistic to the macroscopic, *J. Magn. Magn. Mater.* **242–245**, 116-124 (2002).
- [7] D.C. Jiles and D.L. Atherton, Theory of ferromagnetic hysteresis, *J. Magn. Magn. Mater.* **61**, 48-60 (1986).
- [8] E. C. Stoner, *Ferromagnetism*, Rep. Prog. Phys. **11**, 43-112 (1947).
- [9] S. Talebian, Y. Hojjat, M. Ghodsi, M. R. Karafi and S. Mirzamohammadi, A combined Preisach–Hyperbolic Tangent model for magnetic hysteresis of Terfenol-D, *J. Magn. Magn. Mater.* **396**, 38-47 (2015).
- [10] M. J. Sablik, T. Yonamine and F. J. G. Landgraf, Modeling plastic deformation effects in steel on hysteresis loops with the same maximum flux density, *IEEE Trans. Magn.* **40(5)**, 3219-3226 (2004).
- [11] M. Al Janaideh, S. Rakheja and Chun-Yi Su, A generalized Prandtl–Ishlinskii model for characterizing the hysteresis and saturation nonlinearities of smart actuators, *Smart Mater. Struct.* **18**, 045001 (2009).
- [12] J. Takacs, *Mathematics of Hysteretic Phenomena: The T(x) Model for the Description of Hysteresis*, Wiley-VCH Verlag GmbH & Co. KGaA (2003).
- [13] M. El-Sherbiny, Representation of the magnetization characteristic by a sum of exponentials, *IEEE Trans. Magn.* **9(a)** (1973).
- [14] G. Mörée and M. Leijon, Review of Hysteresis Models for Magnetic Materials, *Energies* **16(9)**, 3908 (2023).
- [15] P. Hejda, Simple representation of magnetic characteristics by smooth functions, *Czech J Phys* **35**, 442–458 (1985).
- [16] J. Rivas, J. Zamarro, E. Martin and C. Pereira, Simple approximation for magnetization curves and hysteresis loops, *IEEE Trans. Magn.* **17(4)** (1981).
- [17] J G.F.T. Widger, Representation of magnetisation curves over extensive range by rational-fraction approximations, *Proceedings of the Institution of Electrical Engineers*, 116(1), 156 – 160 (1969).
- [18] E. Kokornaczyk and M.W. Gutowski, Anhysteretic Functions for the Jiles–Atherton Model, *IEEE Trans. Magn.* **51(2)**, 7300305 (2015).
- [19] R.V. Lapshin, Analytical model for the approximation of hysteresis loop and its application to the scanning tunneling microscope, *Rev. Sci. Instrum.* **66**, 4718 (1995).
- [20] R. R. Kumar, D. D. Mazanek and M. L. Heck, Simulation and Shuttle Hitchhiker validation of passive satellite aerostabilization, *J. Spacecr. Rockets* **32(5)**, 806-811 (1995).
- [21] F. Ossart, L. Hirsinger and R. Billardon, Computation of electromagnetic losses including stress dependence of magnetic hysteresis, *J. Magn. Magn. Mater.*, **196–197**, 924-926 (1999).

- [22] G. Finocchio, M. Carpentieri, E. Cardelli and B. Azzerboni, Analytical solution of Everett integral using Lorentzian Preisach function approximation, *J. Magn. Magn. Mater.* **300(2)**, 451-470 (2006).
- [23] B. Azzerboni, E. Cardelli, E. Della Torre and G. Finocchio, Reversible magnetization and Lorentzian function approximation, *J. Appl. Phys.* **93**, 6635 (2003).
- [24] F. Liorzou, B. Phelps, and D. L. Atherton, Macroscopic Models of Magnetization, *IEEE Trans. Magn.* **36(2)**, 418-428 (2000).
- [25] C.M. Oldenburg, S.E. Borglin and G.J Moridis, Numerical simulation of ferrofluid flow for subsurface environmental engineering applications, *Transp. Porous Media* **38(3)**, 319-344 (2000).
- [26] O. Perevertov, Simple algorithm to estimate mean-field effects from differential permeability minor curves based on the Preisach model, *J. Phys. D: Appl. Phys.* **36**, 785-790 (2003).
- [27] O. Perevertov (2017, May 29-30), Modeling differential susceptibility by Lorentzian [Conference presentation abstract]. 11th International Symposium on Hysteresis Modeling and Micromagnetics (HMM17), Barcelona, Spain.
- [28] O. Perevertov, R. Schaefer, Magnetic properties and magnetic domain structure of grain-oriented Fe-3%Si steel under compression, *Mater. Res. Express* **3**, 096103(1) - 096103(12) (2016).
- [29] O. Perevertov, Influence of the residual stress on the magnetization process in mild steel, *J. Phys. D: Appl. Phys.* **40(4)**, 949-954 (2007).
- [30] O. Perevertov, Application of the Preisach model to the magnetization process in steels, *J. Phys. D: Appl. Phys.* **35**, 2467-2471 (2002).
- [31] O. Perevertov, Describing the effect of tempering on hysteresis curves of 54SiCr6 spring steel by the effective field model, *J. Magn. Magn. Mater.* **324(8)**, 1645-1648 (2012).
- [32] G. Bottoni, D. Candolfo, and A. Cecchetti, Distribution of anisotropy field in recording media deduced from the hysteresis curve, *J. Appl. Phys.* **81**, 3794-3796 (1997).
- [33] O. Perevertov, R. Schaefer, Influence of applied tensile stress on the hysteresis curve and magnetic domain structure of grain-oriented Fe-3% Si steel, *J. Phys. D: Appl. Phys.* **47(18)**, 185001 (2014).
- [34] O. Perevertov, M. Neslušán and A. Stupakov, Detection of milled 100Cr6 steel surface by eddy current and incremental permeance methods, *NDT&E Int.* **87**, 15-23 (2017).
- [35] T. Nakata, N. Takahashi, K. Fujiwara, M. Nakano and Y. Ogura, Accurate measurement method of magnetization curve using ring specimen, *J. Magn. Magn. Mater.* **112**, 71-73 (1992).